DALTON

Gas-phase vibrational spectrum and molecular geometry of $TeCl_4$

Attila Kovács,[a] Kjell-Gunnar Martinsen[b] and Rudy J. M. Konings*[,c]

[a] *Research Group for Technical Analytical Chemistry of the Hungarian Academy of Sciences, Institute of General and Analytical Chemistry, Budapest Technical University, H-1521 Budapest, Hungary*
[b] *Department of Chemistry, University of Oslo, PO Box 1033 Blindern, N-0315 Oslo, Norway*
[c] *Netherlands Energy Research Foundation ECN, PO Box 1, 1755 ZG Petten, The Netherlands*

The gas electron diffraction pattern and the infrared spectrum of gaseous $TeCl_4$ have been measured and *ab initio* molecular orbital calculations performed for the $TeCl_4$ molecule using second-order Møller–Plesset theory (MP2) and a relativistic effective core potential. Applying a scaled quantum mechanical (SQM) method the complete (and up to now the best) force field of the molecule has been evaluated. Based on that SQM force field the complete assignment of the vibrational spectra of $TeCl_4$ has been performed. The electron diffraction analysis resulted in the following geometrical parameters: $r_a(Te–Cl_{ax}) = 243.5(5)$, $r_a(Te–Cl_{eq}) = 229.4(5)$ pm, $Cl_{ax}–Te–Cl_{ax} = 176.4(6)$, $Cl_{eq}–Te–Cl_{eq} = 103.7(7)°$. The molecular geometry is consistent with valence shell electron pair repulsion theory. Comparison with the respective parameters of $Te(CH_3)_4$ supports a previous bonding model for these compounds. Both the computations and the experimental data indicate a much less flexible structure for $TeCl_4$ than was found for $Te(CH_3)_4$.

In the solid state $TeCl_4$ consists of tetrameric units but in the gas phase it is monomeric, as had been shown by Michaelis[1] in 1887. The molecular structure of gaseous $TeCl_4$ was investigated by Stevenson and Shomacher[2] by gas electron diffraction (GED) in 1940. They concluded that it has a trigonal-bipyramidal geometry with a vacant equatorial position (C_{2v} symmetry). The average bond distance in the $TeCl_4$ monomer was found to be 233 ± 2 ppm with $Cl_{ax}–Te–Cl_{ax}$ about 170° and $Cl_{eq}–Te–Cl_{eq}$ between 90 and 120°. However, a model consisting of two different Te–Cl distances (Te–Cl_{ax} 240 and Te–Cl_{eq} 227 pm) could not be excluded.

Raman and infrared spectroscopic studies supported this C_{2v} model.[3,4] Of the total of nine fundamentals for a species of this symmetry, five were found in the Raman and two in the infrared spectrum of the vapour. However, these studies were inconclusive as to the position of the B_2 deformation mode: the original assignment[5] to 100 cm^{-1} was replaced by a dubious shoulder at 130 cm^{-1},[4] indicated however as tentative. The B_1 and A_2 deformation fundamentals around 170 cm^{-1} could not be identified in the Raman spectrum due to possible overlap with the more intense band of the A_1 mode at 158 cm^{-1}. No infrared spectra below 200 cm^{-1} have been recorded for gaseous $TeCl_4$. Infrared investigations of $TeCl_4$ in benzene solutions yielded the value 180 cm^{-1} for the B_1 fundamental.[6]

Ab initio calculations by Novak[7] indicated a trigonal-bipyramidal geometry with two different Te–Cl bond distances. However, in this study, which was performed at the Hartree–Fock level of theory using a non-relativistic basis set for Te, no vibrational analysis was carried out.

In order to complete the description of the molecular properties of $TeCl_4$ we have performed a systematic study using experimental techniques (infrared spectroscopy and gas electron diffraction) as well as *ab initio* molecular orbital methods. Calculations using relativistic effective core potentials (RECPs) for tellurium were considered appropriate because of the computational cost involved in the use of all-electron basis sets and the importance of relativistic effects on heavier elements. Recent calculations using the RECP of Hay and Wadt[8] on $Te(CH_3)_4$ predicted bond lengths within the experimental uncertainty of a high-quality electron diffraction study.[9] In addition, the very low calculated barrier to Berry pseudo-rotation was indicative of the vibrational amplitudes observed in the electron diffraction experiment while the frequencies were in good agreement with those found experimentally.

Table 1 Symmetry coordinates used in the vibrational analysis

Species	Definition*	Description
A_1	$S_1 = 1/\sqrt{2}(\Delta R_1 + \Delta R_2)$	Symmetric axial stretch
	$S_2 = 1/\sqrt{2}(\Delta r_1 + \Delta r_2)$	Symmetric equatorial stretch
	$S_3 = \frac{1}{2}(\Delta\alpha_1 + \Delta\alpha_2 + \Delta\alpha_3 + \Delta\alpha_4)$	Symmetric axial deformation
	$S_4 = \Delta\beta$	Equatorial deformation
A_2	$S_5 = \frac{1}{2}(\Delta\alpha_1 - \Delta\alpha_2 - \Delta\alpha_3 + \Delta\alpha_4)$	Asymmetric axial deformation
B_1	$S_6 = 1/\sqrt{2}(\Delta R_1 - \Delta R_2)$	Asymmetric axial stretch
	$S_7 = \frac{1}{2}(\Delta\alpha_1 + \Delta\alpha_2 - \Delta\alpha_3 - \Delta\alpha_4)$	Asymmetric axial deformation
B_2	$S_8 = 1/\sqrt{2}(\Delta r_1 - \Delta r_2)$	Asymmetric equatorial stretch
	$S_9 = \frac{1}{2}(\Delta\alpha_1 - \Delta\alpha_2 + \Delta\alpha_3 - \Delta\alpha_4)$	Asymmetric axial deformation

* For the definition of internal coordinates see Fig. 1.

Computational Details

The *ab initio* molecular orbital calculations were performed using the GAUSSIAN 94 series of programs.[10] Geometry optimization and the computation of vibrational frequencies were carried out using standard gradient techniques at the second-order Møller–Plesset (MP2) level of theory,[11] with the frozen-core approximation. A double-ζ valence basis set was used for tellurium, in combination with the RECP of Hay and Wadt.[8] The standard 6-31G* basis set was used for chlorine and a single set of d-type polarization functions[12a] was added for tellurium.

To obtain the force constants the first and second derivatives of the potential energy with respect to nuclear coordinates were calculated analytically for the fully optimized geometry. The Cartesian force field was transformed with a set of symmetry coordinates using the computer program TRA3.[12b] The symmetry coordinates are defined in Table 1. To obtain the scaled harmonic force field, frequencies, total energy distribution[13] and vibrational amplitudes of $TeCl_4$ the program SCALE3[14]

Table 2 Vibrational properties of $TeCl_4$; wavenumbers in cm^{-1}, activities expressed as $(I/I_0) \times 100$, where I_0 is the activity of the strongest band

	Wavenumber						
	Experimental		Computed[a]		Computed activity		
	Ref. 4	This study	Unscaled	Scaled[b]	Raman[c]	Infrared[a]	Assignment[d]
A_1	382 Raman		385	384	73	8	94% S_2
	290 Raman		291	285	100	1	95% S_1
	158 Raman[e]		163	152	8	4	56% S_4, 43% S_3
	72 Raman[e]		85	78	4	1	43% S_4, 57% S_3
A_2			166	150	14	0	100% S_5
B_1	314 IR	312 IR	322	317	2	100	100% S_6
		165 IR	183	166	10	2	100% S_7
B_2	382 IR	378 IR	376	376	33	23	100% S_8
	130 Raman	104 IR	113	103	<1	3	100% S_9

[a] At the MP2 level of theory using a 6-31G* basis set for Cl and the RECP of Hay and Wadt[8] for Te. [b] Optimized scale factors for the symmetry-adapted force field: 0.969 (S_1, S_6), 1.006 (S_2, S_8), 0.891 (S_4) and 0.829 (S_3, S_5, S_7, S_9). [c] At the RHF/3-21G* level. [d] Total energy distribution[13] in terms of symmetry coordinates. Only contributions above 10% are given. [e] Tentative assignment:[4] 158 (Raman), equatorial deformation; 72 cm^{-1} (Raman), axial deformation.

was used. For the scaling scheme Pulay's standard scaling method[15] has been adopted, in which the theoretical (unscaled) force constant matrix F has to be subjected to the congruent transformation $F' = T^{\frac{1}{2}}FT^{\frac{1}{2}}$ (where F' is the scaled force-constant matrix and T the diagonal matrix containing the scale factors t_i).[16] The atomic masses used for generation of the G inverse kinetic energy matrix and for calculation of the mean-square vibrational amplitudes were as follows: Te, 127.60; Cl, 35.453.

Raman activities have been calculated with the restricted Hartree–Fock (RHF) method using a 3-21G* basis set as implemented in GAUSSIAN 94.

Experimental

The $TeCl_4$ samples for the measurements in Petten and Oslo were obtained from Aldrich (stated purity 99%) and used without further purification.

Infrared spectroscopy

The infrared spectra were recorded between 425 and 675 K with a BOMEM DA3.02 Fourier-transform spectrometer equipped with an optical gas cell (HTOC-2). Details of the equipment have been described previously.[17,18] The following experimental arrangements were used for the operation of the spectrometer: for the 1000–375 cm^{-1} range a globar light source and a DTGS detector; for the 375–70 and 100–25 cm^{-1} ranges a mercury light source and a helium-cooled germanium bolometer operating at 4.2 or 1.6 K respectively. The spectra were recorded at 0.5 or 1 cm^{-1} resolution; 128 scans were co-added. The gas atmosphere in the cell was argon at a pressure of 15 mbar (1500 Pa) at room temperature.

Gas electcron diffraction

The gas electron diffraction data for $TeCl_4$ were recorded on a Balzer Eldigraph KDG-2 instrument[19] with an inlet system of stainless steel.[20] Sample and nozzle temperatures were 476 ± 3 K, corresponding to a vapour pressure of about 0.3 kPa. However, at this temperature decomposition into $TeCl_2$ and Cl_2 has to be taken into account.[21,22]

Structure refinements were based on four plates obtained with a nozzle-to-plate distance of 50 cm (s from 25.00 to 145.00 nm^{-1} with an increment $\Delta s = 1.25$ nm^{-1}) and four plates obtained with a nozzle-to-plate distance of 25 cm (s from 45.00 to 270.00 nm^{-1} with an increment $\Delta s = 2.50$ nm^{-1}). Optical densities were recorded on a Joyce–Loble densitometer and processed by standard procedures.[23,24] Atomic scattering factors were taken from refs. 25 and 26. Backgrounds were drawn as seventh- (50 cm) or ninth-degree (25 cm) polynomials to the

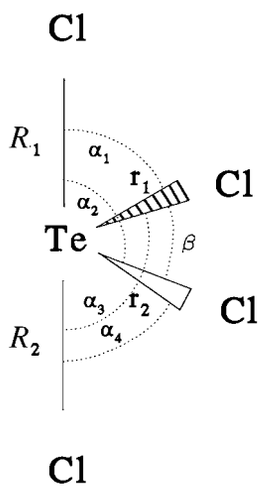

Fig. 1 The C_{2v} model of $TeCl_4$ described by internal coordinates $R_1 = R_2$, $r_1 = r_2$, $\alpha_1 = \alpha_2 = \alpha_3 = \alpha_4$ and β

difference between total experimental intensities and calculated molecular intensities.[27] The resulting molecular intensity curves are displayed in Fig. 2.

Results

Molecular orbital calculations

In order to derive a reliable force field, quantum-chemical calculations have been performed at the MP2 level using the RECP of Hay and Wadt[8] for tellurium. As implemented in GAUSSIAN 94, this level gives qualitative information on the IR intensities but lacks the Raman activity. This latter property was computed at the restricted Hartree–Fock level using a 3-21G* basis set for both tellurium and chlorine. The computed vibrational parameters are shown in Table 2 together with the experimental frequencies. From the results of the RHF/3-21G* calculations only the Raman activities are used in the following discussion. The vibrational frequencies obtained by this method are available from the authors upon request.

To correct for the systematic errors of the quantum-chemical method the scaled quantum mechanical (SQM) force field[28] of $TeCl_4$ was evaluated. Four scale factors were determined for the different types of vibrations: 0.969 (R, axial stretch), 1.006 (r, equatorial stretch), 0.829 (α, axial deformation) and 0.891 (β, equatorial deformation, *cf.* Fig. 1). In the optimization procedure eight experimental frequencies were used, including the bands at 165 and 104 cm^{-1} as obtained in the present study (see below). The root-mean-square (r.m.s.) deviation between the

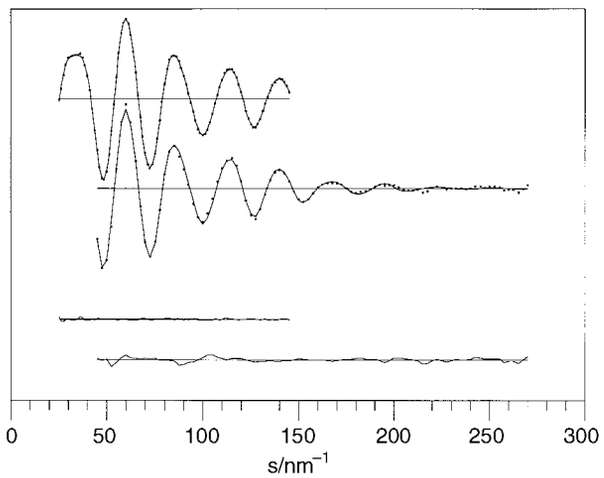

Fig. 2 Experimental modified molecular intensity curves (·) for $TeCl_4$ obtained with nozzle-to-plate distances of 50 and 25 cm, and the modified molecular intensity curves (—) calculated for C_{2v} symmetry. The difference curves are shown below

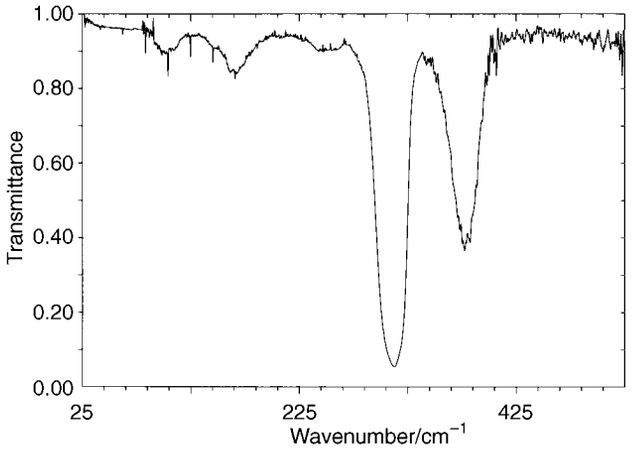

Fig. 3 Infrared spectrum of $TeCl_4$ in the gas phase

experimental and SQM frequencies was 4.3 cm^{-1} while the largest deviation is 6 cm^{-1}. Since the standard scaling method of Pulay[15] is invariant to transformations mixing internal coordinates with the same scaling factor, the scale factors above may be used for both the internal coordinate space (*cf.* Fig. 1) and the symmetry coordinate space (*cf.* Table 1) of $TeCl_4$.

Vibrational analysis

The normal vibrations of a C_{2v} type XY_4 molecule are represented by $\Gamma_{mol} = 4A_1 + A_2 + 2B_1 + 2B_2$, all the modes being Raman and infrared active except for A_2 which is Raman active only.

The gas-phase infrared spectrum of $TeCl_4$ in the range 25–525 cm^{-1} is shown in Fig. 3. Five absorption maxima were observed at 378, 312, 246, 165 and 104 cm^{-1} (Table 2). Their intensities were strongly temperature dependent, suggesting that they are due to gaseous $TeCl_4$ species, except for the band at 246 cm^{-1} which is probably due to a condensation of a species in the infrared beam. The possibility of the presence of lower-valent tellurium chlorides in the gas phase was also considered. Tellurium tetrachloride is known to be monomeric in the gas phase[1,4,29] but mass spectrometric investigations found $TeCl_2$ as a minor contaminant.[4] The vibrational bands of gaseous $TeCl_2$ were reported to be at 377 and 125 cm^{-1}, respectively.[30] While the band at 377 cm^{-1} might partly overlap with our high-intensity band at 378 cm^{-1}, no absorption could be detected at 125 cm^{-1} in our spectra.

The positions of the two higher-frequency bands are in agreement with earlier reports for the B_1 and B_2 stretching fundamentals measured in the IR spectra of the vapour.[4] Previous normal coordinate analyses[5,31] proposed three fundamentals in the range 140–180 cm^{-1} of which the A_1 deformation fundamental was assigned[4] to 158 cm^{-1} on the basis of polarized Raman studies. Since the A_2 mode is Raman active only, the candidates for the band at 165 cm^{-1} in the infrared spectrum are the two infrared-active normal modes (A_1 and B_1 deformations) alone or an overlap of the two. The assignment of the band at 104 cm^{-1} is not unambiguous either. While an early normal coordinate analysis proposed the B_2 deformation to be at 100 cm^{-1},[5] Beattie *et al.*[4] assigned this fundamental to a shoulder at 130 cm^{-1} found in the Raman spectra of the vapour.

On the basis of the results of the molecular orbital calculations we can assign the band at 104 cm^{-1} found in our IR spectra unambiguously to the B_2 deformation mode. This assignment is supported by the calculated pure theoretical and empirically corrected SQM frequencies, which are closer to (the latter even exactly matches) our measured value. Test calculations with the SCALE3 program, in which the band at 130 cm^{-1} was considered instead of that at 104 cm^{-1}, resulted in a much worse root-mean-square deviation (10 cm^{-1}) and in a maximum deviation of 18 cm^{-1}. Another support for our assignment is the calculated Raman activity for the B_2 mode. It was calculated to be very low compared to the Raman activities of the other modes, thus it may be very difficult to observe this normal mode in the Raman spectra. In contrast, a low but detectable infrared intensity was calculated for this mode, in agreement with the observation of the band at 104 cm^{-1} in our spectra.

The band at 165 cm^{-1} in our spectrum has the most complex structure among all the measured ones, which may be ascribed either to a rotation-vibrational structure or to the overlapping of A_1 and B_1 vibration bands. However, the interference of both effects should also be considered. Badger and Zumwalt[32] calculated the theoretical band envelopes for different types of unsymmetrical rotors, grouped according to the relative magnitude of their three principal moments of inertia. The band shapes of our spectra are in good agreement with their respective presentations (see Figs. 2–4, $S = -\frac{1}{2}$, $r = \frac{3}{4}$ blocks, in the paper by Badger and Zumwalt[32]) considering that the separation of the maxima of the P and R branches of only a few cm^{-1} for $TeCl_4$ may be readily obscured by hot bands at the (high) temperatures of our measurements.

In the Raman spectra[3] the band at 158 cm^{-1} is superimposed on a much broader band of about the same wavenumber (the middle being shifted by 5–10 cm^{-1} to higher values where our band at 165 cm^{-1} lies). During the polarization measurement the former band was not observed (on that basis it was assigned to the A_1 species) while the broad one remained. This latter band may be the depolarized part of A_1 eventually superimposed with the B_1 and A_2 deformation modes. As the shape of the band at 165 cm^{-1} in the infrared spectrum seems to be symmetric and no distortion can be observed at its 158 cm^{-1} side, this band is assigned to the B_1 deformation mode.

On the basis of the present information we cannot make accurate assignments for the A_2 fundamental. However, based on the good performance of our SQM force field for the other fundamentals we propose that it is with highest probability within ±10 cm^{-1} of the SQM value.

The fundamentals are characterized by their total energy distribution[13] as shown in Table 2. It can be seen that only two normal modes, the two A_1 deformations, are strongly mixed. All the other ones proved to be practically pure. The complete SQM force field (the best quality force field up to now) for $TeCl_4$ in the internal coordinates (*cf.* Fig. 1) is presented in Table 3. For comparison, the modified valence force field (MVFF) derived by Ozin and Vander Voet[5] is also included. In general, there is satisfactory agreement between the force constants related to stretching (except for f_{RR}), however the MVFF force

Table 3 Force field of $TeCl_4$; units are N m^{-1} (f_R, f_{RR}, f_r, f_{rr} and f_{Rr}), N rad^{-1} (f_{Ra}, f_{ra}, $f_{R\beta}$ and $f_{r\beta}$) and N m rad^{-2} (f_a, f_{aa}, f_β and $f_{a\beta}$) (1 N m^{-1} = 100 mdyn $Å^{-1}$). See Fig. 1 for the definition of internal coordinates

	MVFF[a]	SQM	Characterization
f_R	170.0	157.5	
f_{RR}	5.0	18.3	
f_r	235.0	235.5	
f_{rr}	12.0	10.5	
f_{Rr}	10.0	12.0	
f_α	16.6×10^{-20}	94.1×10^{-20}	
$f_{\alpha\alpha}$[b]	1.7×10^{-20}	7.8×10^{-20}	Common *r*, *e.g.* $\alpha_1 - \alpha_3$
		13.3×10^{-20}	Common *R*, *e.g.* $\alpha_1 - \alpha_2$
		9.6×10^{-20}	No common bond, *e.g.* $\alpha_1 - \alpha_4$
$f_{R\alpha}$[b]	8.6×10^{-10}	3.0×10^{-10}	Common *R*, *e.g.* $R_1 - \alpha_1$
		-11.3×10^{-10}	No common *R*, *e.g.* $R_1 - \alpha_3$
$f_{r\alpha}$[b]	2.8×10^{-10}	10.5×10^{-10}	Common *r*, *e.g.* $r_1 - \alpha_1$
		1.3×10^{-10}	No common *r*, *e.g.* $r_1 - \alpha_2$
f_β	12.9×10^{-20}	63.5×10^{-20}	
$f_{\alpha\beta}$	1.8×10^{-20}	15.5×10^{-20}	
$f_{R\beta}$		-0.5×10^{-10}	
$f_{r\beta}$	2.8×10^{-10}	2.9×10^{-10}	

[a] Modified valence force field by Ozin and Vander Voet.[5] [b] In contrast to the empirical treatment by Ozin and Vander Voet[5] the *ab initio* calculations resulted in different interaction force constants depending on the way of combination of the individual internal coordinates.

Table 4 Amplitudes and thermal correction parameters calculated from the SQM force field; vibrational amplitudes (*l*) and vibrational correction terms (*D*) in pm

Parameter	*l*	*D*
Te–Cl_{ax}	6.8	−0.9
Te–Cl_{eq}	5.6	−0.5
$Cl_{eq} \cdots Cl_{eq}$	17.0	0.4
$Cl_{eq} \cdots Cl_{ax}$	15.4	−0.4
$Cl_{ax} \cdots Cl_{ax}$	9.0	−0.2

Table 5 Results from the GED analysis; distances (r_a), r.m.s. vibrational amplitudes (*l*) in pm and angles in °. Values in parentheses are the estimated uncertainties * in units of the last digit; *x* denotes the mole fraction

			D term included	
Parameter	r_a	*l*	r_a	*l*
Te–Cl_{ax}	243.0(6)	8.2(7)	243.5(5)	7.6(7)
Te–Cl_{eq}	229.8(6)	7.4(6)	229.4(5)	6.9(6)
$Cl_{eq} \cdots Cl_{eq}$	330.7(5)	13.9(6)	330.7(6)	13.7(6)
$Cl_{eq} \cdots Cl_{ax}$	360(1)	12(2)	360(1)	12(2)
$Cl_{ax} \cdots Cl_{ax}$	486(1)	11(1)	485(1)	11(1)
Cl_{ax}–Te–Cl_{ax}	175.9(6)		176.4(6)	
Cl_{eq}–Te–Cl_{eq}	103.0(7)		103.7(7)	
x ($TeCl_2$)	0.16(7)		0.18(6)	
R factor (50/25), total	(2.05/7.73) 3.27		(2.03/7.67) 3.24	

* See text.

constants related to bending are in considerable disagreement with the present results. From the paper of Ozin and Vander Voet it is not clear how they treated the different types of $f_{\alpha\alpha}$, $f_{R\alpha}$ and $f_{r\alpha}$ interaction force constants (*cf.* Table 3). Our results show that they cannot be either neglected or arbitrarily assigned the same value.

Structure refinement

The results of the molecular orbital calculations clearly show that $TeCl_4$ has a C_{2v} structure. Our refinement of $TeCl_4$ was therefore based on a model with two independent bond distances *r*($TeCl_{ax}$) and *r*($TeCl_{eq}$) and two independent bond angles

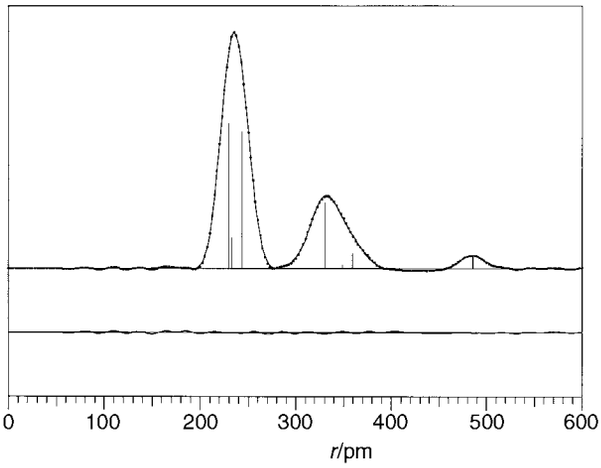

Fig. 4 Experimental (·) and calculated (−) radial distribution curves for $TeCl_4$; the vertical bars indicate the contributions of the various bond distances in $TeCl_4$ [r_a(Te–Cl_{eq}) = 229.4, r_a(Te–Cl_{ax}) = 243.5, r_a($Cl_{eq} \cdots Cl_{eq}$) = 330.7, r_a($Cl_{eq} \cdots Cl_{ax}$) = 360, r_a($Cl_{ax} \cdots Cl_{ax}$) = 485 pm] and in $TeCl_2$ [r_a(Te–Cl) = 232.9, r_a(Cl ⋯ Cl) = 349 pm] to the scattering function. The difference curve is given below. Artificial damping constant k = 15 pm^2

Cl_{ax}–Te–Cl_{ax} and Cl_{eq}–Te–Cl_{eq}. This gives four parameters to refine along with two bonded and three non-bonded root-mean-square amplitudes (*l*).*

Owing to partial decomposition some $TeCl_2$ and Cl_2 might have been present in the vapour in detectable amounts.[4] Therefore an exploratory refinement was done to seek for the presence of these species. The amount of $TeCl_2$ was refined with the geometrical parameters r_a(Te–Cl) = 232.9, *l*(Te–Cl) = 7.0 pm, r_a(Cl ⋯ Cl) = 349 and *l*(Cl ⋯ Cl) = 15.2 pm,[33] the amount of Cl_2 with r_a(Cl–Cl) = 200 and l = 5.2 pm.[34] Initially the amounts of Cl_2 and $TeCl_2$ were refined together but it was found that Cl_2 was not present in detectable amounts and hence it was excluded from the final refinements. The difference in the concentrations of Cl_2 and $TeCl_2$ is most likely due to the fact that some decomposition had occurred before the diffraction pattern was recorded. Owing to its high volatility, the Cl_2 gas escaped immediately whereas the $TeCl_2$ might remain as a condensed phase, vaporizing when the temperature was raised further.

The correction term for thermal vibrations, $D = r_\alpha - r_a$, for the GED refinement was calculated from the SQM force field listed in Table 3 by the program ASYM 20.[35] The resulting values, Table 4, were used to carry out refinement on a geometrically consistent r_α structure. The result of this refinement is given in Table 5 under the heading *D* term included. The two sets of parameters agree within the error limits, indicating that the effect of shrinkage is negligible at the temperature of our measurements.

The refinement was carried out by least-squares calculations on the molecular intensity curves using the program KCED 26.[36,37] Since the refinement was carried out with a diagonal weight matrix, the estimated standard deviation, σ_{LS}, computed by the program, has been multiplied by a factor of 2 to include the additional uncertainty due to data correlation,[38] and further expanded to include an estimated scale uncertainty of 0.1%. Structure refinements of the two bond distances, the two valence angles and all the r.m.s. amplitudes along with the mole fraction of $TeCl_2$ converged to yield the best values listed in Table 5, irrespectively of the relative magnitude of the axial and equatorial bond distance in the starting model. The corresponding radial distribution curve is shown in Fig. 4. The two

* Alternatively a model with one Te–Cl distance and the difference between the axial and equatorial bond as independent parameters can be used. Refinements of such a model proceeded without difficulties and gave the same results as reported in Table 5, as is expected.

Table 6 Comparison of $TeCl_4$ and $Te(CH_3)_4$; bond lengths in pm, angles in °

	$TeCl_4$				
	This study			$Te(CH_3)_4$[9]	
Parameter	r_a	Calc.	Calc.[7]	r_a	Calc.*
$Te–L_{ax}$	243.5(5)	244.1	246.1	226.9(6)	225.6
$Te–L_{eq}$	229.4(5)	231.3	232.0	213.8(5)	214.2
$L_{ax}–Te–L_{ax}$	176.4(6)	176.6	173.0	153(2)	158.7
$L_{eq}–Te–L_{eq}$	103.7(7)	100.2	101.6	118(3)	111.6

* The difference between the calculated and experimental bond angles of $Te(CH_3)_4$ may be attributed to the fact that a thermal average structure is obtained in the GED measurement.[39]

bonded distances were correlated with a coefficient of −0.76, the two bonded amplitudes with 0.78. In addition there were correlations between the bonded distances and their amplitudes, the highest being 0.93 between the equatorial bond distance and its r.m.s. amplitude. The uncertainty due to correlation of the parameters is included in the calculation of σ_{LS}.

When the structure was refined without inclusion of the mole fraction of $TeCl_2$ we obtained an *R* factor of 3.43 and the same parameters as in Table 5 except for $Cl_{ax}–Te–Cl_{ax}$ which became 178.5(6)°. Though inclusion of the mole fraction of $TeCl_2$ does not change the fit, the uncertainty due to decomposition is reflected in the estimation of the uncertainties of the geometric parameters.

The values for the structure parameters obtained by the GED investigation are in good agreement with the corresponding calculated ones (MP2 level), as summarized in Table 6. Comparing the values for the amplitudes calculated from the SQM force field (*l* in Table 4) with their experimental counterpart (*l* in Table 5) we note that the values for the bonded amplitudes thus obtained are about one or two times the estimated uncertainty higher than the calculated ones. In view of the dynamic nature of tetrasubstituted Te [*cf*. Berry pseudo-rotation in $Te(CH_3)_4$, as described by Blake *et al*.[9]], this is in the range expected. Such disagreement might be removed if the dynamic nature of the molecule was to be modelled more explicitly as pointed out by Samdal.[40] However, we believe the disagreement is too small to follow a dynamic approach. This is supported by our theoretical calculations at the MP2 level, which predicted the barrier for pseudo-rotation for $TeCl_4$ to be 30.9 kJ mol^{-1}. Two of the non-bonded amplitudes are calculated to be higher than those obtained in the GED investigation. Hedberg[41] has suggested that this happens when a harmonic model is used for the calculation of the amplitudes.

Discussion

The molecular geometry of $TeCl_4$ is completely consistent with valence shell electron pair repulsion (VSEPR) theory.[42] In a trigonal-bipyramidal arrangement the five electron-pair domains are not all equivalent. In particular, the axial positions are more crowded than the equatorial ones. Thus, to minimize overlap with the neighbours, the axial bond distances are longer than the equatorial ones. Since more space is available in the valence shell in an equatorial position, the larger lone pair occupies preferentially an equatorial position. The larger space requirement of the lone pair is also indicated by the $Cl_{eq}–Te–Cl_{eq}$ angle being smaller than 120° and in the tilt of the axial chlorines towards the equatorial ones.

Also Musher[43] has outlined a bonding model for compounds such as $TeCl_4$ and $Te(CH_3)_4$. The general concern of this model is the concept of hypervalent bonds. It is proposed that hypervalent compounds are using only s and p orbitals in bond formation, *i.e.* d orbitals play a negligible role. This results in two different kinds of bonds in hypervalent compounds, where one set is more or less identical (at least with respect to bond length) as in group valent compounds.[44] The other set of bonds is called hypervalent and is constituted by three-centre four-electron bonding (3c-4e). This picture is now generally accepted and recent comments on the implications of the concept and the effect of electronegative ligands can be found in refs. 45–47.

If we compare the Te–Cl bond length in the $TeCl_4$ molecule with that in $TeCl_2$, $r_a = 232.9(3)$ pm,[33] there is a relative reduction (3 pm) in the equatorial bond distance and a relative elongation of the axial bond distance (10 pm). The latter elongation is that expected from the 3c-4e concept. The shortening of the equatorial bond (which is termed a 'normal' covalent bond) is that expected when electronegative ligands are added, thereby increasing the partial positive charge on the central atom.

For the methyl analogue $Te(CH_3)_4$ we may make the same comparison. The Te–C bond distance in $Te(CH_3)_2$ is 214.2(5) pm.[48] We do not see any shortening of the equatorial bond in $Te(CH_3)_4$, $r_{eq} = 213.8(5)$ pm,[9] but there is a slightly larger elongation (13 pm) of the axial bond relative to $Te(CH_3)_2$. Again this observation is in agreement with the concept of 3c-4e bonding. Here there is no electronegative ligand to induce a shortening of the covalent bonds in the equatorial plane.

This discussion can be extended to the structure of solid compounds. That of $TeCl_4$ is tetrameric whereas that of $Te(CH_3)_4$ is monomeric; solid $TeCl_2(CH_3)_2$ has a chain structure with the chlorine atom in bridging position. In the molecular unit of $TeCl_2(CH_3)_2$ the shortest set of Te–Cl distances has a mean of 251.5 pm and the average Te–C distance is 211.4(2) pm.[49] In relation to the 3c-4e concept we would expect the Te–C distance in $TeCl_2(CH_3)_2$ to be shorter than the equatorial Te–C distance in $Te(CH_3)_4$ due to the replacement of the methyl groups in axial position with the more electronegative chlorine atom. This is exactly what is found. In the same sense the axial Te–Cl distance would be expected to be longer in $TeCl_2(CH_3)_2$ than we observe in monomeric $TeCl_4$ due to the absence of electronegative chlorine in the equatorial position. This is also in agreement with the present results.

Acknowledgements

We thank Professors G. I. Csonka, A. Haaland and M. Hargittai for helpful discussions and Ing. A. S. Booij, Ing. S. Gundersen and H. V. Volden for technical assistance. A. K. acknowledges the Hungarian–Netherlands Cultural Exchange programme for a fellowship and the Hungarian National Scientific Research Foundation (OTKA, No. T 014073) for support.

References

1 A. Michaelis, *Ber. Deutsch. Chem. Ges*., 1887, **20**, 1780.
2 P. D. Stevenson and V. Schomacher, *J. Am. Chem. Soc*., 1940, **62**, 1267.
3 I. R. Beattie, J. R. Horder and P. J. Jones, *J. Chem. Soc. A*, 1970, 329.
4 I. R. Beattie, O. Bizri, H. E. Blayden, S. B. Brumbach, A. Bukovszky, T. R. Gilson, R. Moss and B. A. Phillips, *J. Chem. Soc., Dalton Trans*., 1974, 1747.
5 G. A. Ozin and A. Vander Voet, *J. Mol. Struct*., 1971, **10**, 397.
6 D. M. Adams and P. J. Lock, *J. Chem. Soc. A*, 1967, 145.
7 I. Novak, *Heteroat. Chem*., 1992, **3**, 431.
8 P. J. Hay and W. R. Wadt, *J. Chem. Phys*., 1985, **82**, 270; W. R. Wadt and P. J. Hay, *J. Chem. Phys*., 1985, **82**, 284; P. J. Hay and W. R. Wadt, *J. Chem. Phys*., 1985, **82**, 299.
9 A. J. Blake, C. R. Pulham, T. M. Greene, A. J. Downs, A. Haaland, H. P. Verne, H. V. Volden, C. J. Marsden and B. A. Smart, *J. Am. Chem. Soc*., 1994, **116**, 6043.
10 M. J. Frisch, G. W. Trucks, H. B. Schlegel, P. M. W. Gill, B. G. Johnson, M. A. Robb, J. R. Cheeseman, T. Keith, G. A. Petersson, J. A. Montgomery, K. Raghavachari, M. A. Al-Laham, V. G. Zakrzewski, J. V. Ortiz, J. B. Foresman, J. Cioslowski, B. B. Stefanov, A. Nanayakkara, M. Challacombe, C. Y. Peng, P. Y. Ayala, W. Chen, M. W. Wong, J. L. Andres, E. S. Replogle, R.

Gomperts, R. L. Martin, D. J. Fox, J. S. Binkley, D. J. Defrees, J. Baker, J. P. Stewart, M. Head-Gordon, C. Gonzalez and J. A. Pople, GAUSSIAN 94, Revision B.2, Gaussian Inc., Pittsburgh, PA, 1995.
11 C. Møller and M. S. Plesset, *Phys. Rev*., 1934, **46**, 618.
12 (*a*) B. A. Smart and C. H. Schiesser, *J. Comput. Chem*., 1995, **16**, 1055, (*b*) J. M. Coffin and P. Pulay, TRA3, University of Arkansas, 1989.
13 P. Pulay and F. Török, *Acta Chim. Hung*., 1965, **47**, 273.
14 G. Pongor, G. Fogarasi, I. Magdó, J. E. Boggs, G. Keresztury and I. S. Ignatyev, *Spectrochim. Acta, Part A*, 1992, **48**, 111.
15 P. Pulay, in *Applications of Electronic Structure Theory, Modern Theoretical Chemistry*, ed. H. F. Schaefer III, Plenum, New York, 1977, vol. 4, p. 153.
16 V. I. Pupyshev, Yu. N. Panchenko, C. W. Bock and G. Pongor, *J. Chem. Phys*., 1991, **94**, 1247.
17 R. J. M. Konings, A. S. Booij and E. H. P. Cordfunke, *Vibr. Spectrosc*., 1991, **1**, 383.
18 R. J. M. Konings and A. S. Booij, *J. Chem. Thermodyn*., 1992, **24**, 1181.
19 W. Zeil, O. Graber and L. Wegmann, *Z. Instrumentenkd*., 1966, **74**, 84; O. Bastiansen, R. Graber and L. Wegmann, *Balzers High Vac. Rep*., 1969, **25**, 1.
20 K.-G. Martinsen and H. V. Volden, Annual Report, The Norwegian Electron Diffraction Group, 1993.
21 H. Oppermann, G. Stöver and E. Wolf, *Z. Anorg. Allg. Chem*., 1974, **410**, 179.
22 S. A. Ivashin and E. S. Petrov, *Izv. Sib. Otd. Akad. Nauk. SSSR, Ser. Khim. Nauk*, 1970, 48 (*Sib. Chem. J*., 1970, 609).
23 S. Gundersen, T. G. Strand and H. V. Volden, *J. Appl. Crystallogr*., 1992, **25**, 409.
24 S. Gundersen, T. G. Strand and H. V. Volden, *J. Mol. Struct*., 1995, **346**, 121.
25 A. W. Ross and M. Fink, *J. Chem. Phys*., 1986, **85**, 6810.
26 *International Tables of X-Ray Crystallography*, ed. A. J. C. Wilson, Kluwer, Dordrecht, 1992, vol. C, p. 245.
27 G. Gundersen and S. Samdal, KCED 12, University of Oslo, 1980.
28 P. Pulay, G. Fogarasi, G. Pongor, J. E. Boggs and A. Vargha, *J. Am. Chem. Soc*., 1983, **105**, 7037.
29 J. H. Simons, *J. Am. Chem. Soc*., 1930, **52**, 3488.
30 I. R. Beattie and R. O. Perry, *J. Chem. Soc. A*, 1970, 2429.
31 S. J. Cyvin, B. N. Cyvin, W. Brockner and A. F. Demiray, *Z. Naturforsch., Teil A*, 1978, **33**, 714.
32 R. M. Badger and L. R. Zumwalt, *J. Chem. Phys*., 1938, **6**, 711.
33 L. Fernholt, A. Haaland and H. V. Volden, *J. Mol. Struct*., 1985, **125**, 29.
34 A. Haaland, A. Hammel, K.-G. Martinsen, J. Tremmel and H. V. Volden, *J. Chem. Soc., Dalton Trans*., 1992, 2209.
35 L. Hedberg and I. M. Mills, *J. Mol. Spectrosc*., 1993, **160**, 117.
36 B. Andersen, H. M. Seip, T. G. Strand and R. Stølevik, *Acta Chem. Scand*., 1969, **23**, 3224.
37 G. Gundersen, S. Samdal and H. M. Seip, KCED 26, University of Oslo, 1980.
38 H. M. Seip, T. G. Strand and R. Stølevik, *Chem. Phys. Lett*., 1969, **3**, 617.
39 H. P. Verne, personal communication; see also ref. 9.
40 S. Samdal, *J. Mol. Struct*., 1994, **318**, 131.
41 L. Hedberg, *J. Phys. Chem*., 1982, **86**, 593.
42 R. J. Gillespie and I. Hargittai, *The VSEPR Model of Molecular Geometry*, Allyn and Bacon, London, 1991.
43 J. I. Musher, *Angew. Chem*., 1969, **81**, 68.
44 A. Haaland, *J. Mol. Struct*., 1983, **97**, 115.
45 A. Haaland, A. Hammel, K. Rypdal, O. Swang, J. Brunvoll, O. Gropen, M. Greune and J. Weidlein, *Acta Chem. Scand*., 1993, **47**, 368.
46 A. Haaland, H. P. Verne, H. V. Volden and C. R. Pulham, *J. Mol. Struct*., 1996, **376**, 151.
47 J. Kadel and H. Oberhammer, *Inorg. Chem*., 1994, **33**, 3197.
48 R. Blom, A. Haaland and R. Seip, *Acta Chem. Scand., Ser. A*, 1983, **37**, 595.
49 R. F. Zigla and J. M. Trop, *J. Am. Chem. Soc*., 1983, **105**, 299.

Received 9*th August* 1996; *Paper* 6/05574E